Biomedicine & Pharmacotherapy 191 (2025) 118549

Contents lists available at ScienceDirect

Biomedicine & Pharmacotherapy

journal homepage: www.elsevier.com/locate/biopha

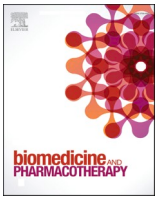

Givinostat inhibits *in vitro* differentiation of cardiac fibroadipogenic precursors from a mouse model of arrhythmogenic cardiomyopathy

Sara Vencato [a], Chiara Romanato [a], Monica Forino [b], Gianluca Fossati [b], Angelo Velle [a], Nicola Facchinello [c], Paola Braghetta [c], Simonetta Andrea Licandro [b], Chiara Romualdi [a], Martina Calore [a], Libero Vitiello [a], Christian Steinkuhler [b,*], Alessandra Rampazzo [a,*]

[a] Department of Biology, University of Padua, Via Ugo Bassi 58/B, Padua 35131, Italy
[b] Preclinical R&D Department, Italfarmaco S.p.A., Via dei Lavoratori, 54 Cinisello Balsamo, Milan 20092, Italy
[c] Department of Molecular Medicine, University of Padua, Via Ugo Bassi 58/B, Padua 35131, Italy

ARTICLE INFO

Keywords:
Arrhythmogenic cardiomyopathy
Sudden death
Drug repurposing
PPAR pathway

ABSTRACT

Arrhythmogenic cardiomyopathy (ACM) is a rare genetic cardiac disease and one of the leading causes of sudden cardiac death in young individuals and athletes. Current treatments focus on preventing arrhythmias and sudden cardiac death, but no effective therapy targeting disease progression is available. Myocardial replacement with fibro-fatty tissue, a hallmark of ACM, is primarily driven by the activation of cardiac fibroadipogenic precursors (cFAPs). Here, we evaluate the efficacy of a pan inhibitor of histone deacetylases (givinostat) in reducing cFAP proliferation and differentiation. These cells were found to be enriched in the hearts of a transgenic ACM murine model (Tg-hQ), which overexpresses the DSG2 p.Q558* mutation, compared to wild-type (WT) controls. We observed that givinostat reduced the proliferation of both Tg-hQ and WT isolated cFAPS. Additionally, cFAPS were induced to differentiate into adipocytes or fibroblasts and treated with givinostat. The drug treatment led to a reduction in the number of adipocytes under pro-adipogenic conditions. RNA sequencing analysis revealed a significant downregulation of key regulators of adipogenic differentiation and lipid metabolism (*Pparg*, *Cebpa* and *Adipoq*). In parallel, cells cultured under pro-fibrotic conditions showed decreased expression of genes encoding components of the extracellular matrix (*Col1a1*, *Col6a1* and *Postn*) upon givinostat treatment. Overall, these results support the potential of givinostat in modulating cFAP proliferation and differentiation *in vitro*, warranting further *in vivo* studies to assess its impact on fibro-fatty tissue replacement in ACM.

1. Introduction

Arrhythmogenic cardiomyopathy (ACM) is a genetic cardiac disease characterized phenotypically by structural and functional alterations of the cardiac tissue, with an estimated prevalence of ~1:5.000 individuals [1]. The disease exhibits variable expressivity and reduced, age-related penetrance. Clinical manifestations typically arise during the third to fourth decades of life, and include syncope and ventricular tachycardia, with sudden cardiac death (SCD) often being its initial and sole presentation. The pathological hallmark of ACM is the fibrofatty replacement of myocardial tissue, often associated with ventricular atrophy [2,3]. Histologically, the disease progresses from the subepicardial region towards the endocardium, resulting in a thin, transmural lesion. The subform involving only the right ventricle is the most common, although left and biventricular forms are well-documented [4]. In the right dominant subform, the majority of pathogenic variants are located in three genes, *PKP2*, *DSP*, and *DSG2*, which encode desmosomal proteins [5].

Currently, there are no curative treatments for ACM. Therapeutic strategies focus on attenuating symptoms, slowing disease progression, and preventing SCD [6]. Recent research efforts are focused on the development of gene therapy approaches aimed at restoring functional genes. Notably, studies involving AAV-mediated delivery of the wild-type *PKP2* gene in three distinct ACM murine models demonstrated positive outcomes, halting disease progression or preventing pathological manifestations [7–9]. Although ACM was first described nearly thirty years ago, its pathogenic mechanisms remain incompletely understood. Studies using different animal models point to the

* Corresponding authors.
E-mail addresses: c.steinkuhler@italfarmacogroup.com (C. Steinkuhler), alessandra.rampazzo@unipd.it (A. Rampazzo).

https://doi.org/10.1016/j.biopha.2025.118549
Received 30 May 2025; Received in revised form 9 September 2025; Accepted 10 September 2025
Available online 12 September 2025

involvement of the Wnt/β-catenin signaling in combination with Hippo pathway [10,11]. However, the involvement of additional pathways in ACM pathogenesis has yet to be fully elucidated.

While fibrosis can be observed in various cardiomyopathies, pathological fatty infiltration is a hallmark of ACM. Notably, this fatty involvement results from adipocyte infiltration (adipogenesis) rather than lipid droplet accumulation within other cell types, such as cardiomyocytes (lipogenesis) [12]. Genetic lineage tracing studies in mouse models have shown that cardiac progenitor cells originating from the second heart field and a subset of mesenchymal progenitor-like cells, known as fibroadipogenic progenitors (FAP), may differentiate into adipocytes during the ACM disease process [13]. Recent lineage tracing studies identified PDGFRα$^+$ Sca-1$^+$ heart-resident cells as cardiac fibroadipogenic progenitors (cFAPs), which directly contribute to fibrotic infiltration in a transgenic murine model of ACM (Tg-hQ) previously developed by our group [14]. This model is based on the cardiac-specific overexpression of a mutated human DSG2 gene carrying the c.1672 C>T (p.Q558*) nonsense mutation, originally identified in an ACM patient. Detailed characterization of the Tg-hQ model revealed several hallmark features of the disease, including cardiomyocyte loss, biventricular fibrosis, and a significant reduction in both the size and number of desmosomes [15].

Accumulating evidence highlights the involvement of epigenetic modifications in the initiation and progression of fibrotic replacement in multiple organs. A growing body of research demonstrated dysregulation of histone deacetylases (HDACs) in several pathologies associated with cardiac fibrosis [16]. HDACs are enzymes that play a pivotal role in epigenetic regulation by deacetylating nucleosomal histone tails, thereby modulating gene expression. Beyond their nuclear function, HDACs also deacetylate a range of non-histone proteins involved in diverse cellular processes [17]. *In vitro* and *in vivo* studies have shown that HDAC inhibition can have beneficial effects in preventing or reversing fibrogenesis. In particular, the pan-HDAC inhibitor (HDACi) givinostat proved effective in reducing fibrosis and improving muscle mass and strength in the *mdx* murine model of Duchenne muscular dystrophy (DMD) [18,19]. Moreover, in clinical trials on ambulant DMD patients, givinostat was able to reduce fibrotic and adipose tissue, and to increase muscle fiber size, and achieve the primary end point, with only mild-to-moderate adverse events [20,21]. In March 2024 givinostat received FDA approval for the treatment of young DMD patients [22].

Evidences from several studies also point to FAPs as potential direct targets of HDACis, as these compounds have been shown to inhibit fibro-adipogenic differentiation of FAPs isolated from *mdx* mice [23].

In the cardiac setting, pan and selective HDACis have been shown to reverse myofibroblasts activation, reduce fibrosis, attenuate ventricular remodeling, and preserve cardiac function in different animal models of cardiac hypertrophy and heart failure [16,24]. Additionally, a HDAC2-specific inhibitor has been reported to improve cardiac dysfunction and reduce adverse cardiac remodeling in a rat model of doxorubicin-induced cardiac injury [25]. Given that FAP differentiation could be regulated by epigenetic modifications [23], this study aimed to investigate whether givinostat could influence the fibrogenic and adipogenic potential of cFAPs isolated from Tg-hQ, a transgenic ACM model that recapitulates the main histopathological features of the disease and in which cFAPs directly contribute to fibrous infiltration [14,15].

2. Methods

2.1. Animals

The study was conducted using the Tg-hQ transgenic mouse line, previously generated in our laboratory. This model is characterised by cardiomyocyte-specific overexpression of a human DSG2 gene harboring the c.1672 C>T (p.Q558*) nonsense mutation, under the control of the cardiac-specific mouse α-myosin heavy chain (α-MyHC) promoter. Comprehensive phenotypic characterization of this model has revealed structural and molecular cardiac alterations [15]. Non-transgenic animals from the same original C57BL/6 N strain were used as controls. For heart collection, mice were anesthetized using Iso-Vet isoflurane 2 % in 1 L/minute oxygen flow and euthanized by cervical dislocation at 10 months of age. Hearts were perfused with PBS containing heparin (10 U/mL), the atria were removed, and only the ventricular portion was processed.

All animal procedures were conformed to the guidelines from Directive 2010/63/EU of the European Parliament on the protection of animals used for scientific purposes and to the current NIH guidelines for the Care and Use of Laboratory Animals. All experimental protocols were approved by the internal Animal Research Ethical Committee and by the Italian Ministry of Health regulation (approval number 68/2011).

2.2. Isolation of FAPs from cardiac tissue

cFAPs were isolated from 10-month-old control (WT) and Tg-hQ mice. Freshly dissected hearts were digested for 30 min at 37°C in 2 mg/mL Collagenase II (Sigma) with 2.5 mM $CaCl_2$, followed by a second digestion for 1 h at 37°C in a solution containing 1,5 U/mL Collagenase D (Sigma) and 2.4 U/mL Dispase II (Sigma) in 5 mM $CaCl_2$. The digested material was resuspended in sorting buffer containing 0,5 % w/v BSA and 2 mM EDTA in PBS, dissolved by pipetting, and passed through 70 μm and 40 μm cell strainers. The resulting cell suspension was centrifuged, and the pellet was resuspended in red blood cell lysis buffer for 1 min, followed by washing with sorting buffer. The cell pellet obtained after centrifugation was processed for fluorescence-activated cell sorting (FACS). To minimize variability due to the isolation process, one control and one Tg-hQ mouse were processed and analyzed in parallel for each cell preparation.

2.3. Fluorescence-activated cell sorting (FACS)

Cells were labelled for FACS using a cocktail containing anti-CD31-PE-Cy7 (Thermo Fisher Scientific), anti-CD45-eFluor450 (Thermo Fisher Scientific), anti-PDGFRα-APC (Thermo Fisher Scientific) and anti-Sca1-FITC (Thermo Fisher Scientific). In addition, Viobility™ 405/520 Fixable Dye (Miltenyi Biotec) was used to distinguish live from dead cells. A small volume of the cell suspension was used to generate each FMO (Fluorescence Minus One) control. Stained cells were resuspended in sorting buffer and sorted using a FACSAria™ IIIu cell sorter. Resting and committed cFAPs were identified as CD45$^-$ CD31$^-$ Sca1$^+$ PDGFRα$^+$ and CD45$^-$ CD31$^-$ Sca1$^-$ PDGFRα$^+$ respectively. CD45 and CD31 were used to exclude hematopoietic and endothelial cells, while PDGFRα and Sca-1 were employed to select a cardiac mesenchymal progenitor population. Sorted cells were collected in FBS-pretreated tubes containing DMEM GlutaMAX (Gibco) supplemented with 20 % FBS, penicillin and streptomycin.

2.4. Cell cultures and differentiation

Resting cFAPs were expanded in a proliferation medium with 5 ng/mL FGFβ (Immunotools Gmbh, Germany). To induce adipogenic differentiation, two different media were employed. After an initial three-day incubation in proliferation medium, cells were exposed to the first adipogenic medium (hereafter indicated as AM I) for three days, followed by a second three-day incubation in the second adipogenic medium (hereafter indicated as AM II). For fibroblast differentiation, cells were cultured in proliferation medium for three days, followed by an additional six days in the same medium supplemented with 5 ng/mL TGFβ (PeproTech). Unless otherwise specified, all media and supplements were from Gibco. Where indicated, givinostat (provided by Italfarmaco, Milan, Italy) was added to the different media at a final concentration of 50 nM, based on previously published work from Milan et al. [26]. Equivalent volumes of the vehicle (DMSO) were added to

untreated control conditions.

2.5. Evaluation of cell proliferation and apoptosis

The proliferation rate of cultured cells was evaluated using the Click-iT® EdU Imaging Kit (Invitrogen) according to the manufacturer's protocol. Briefly, cFAPs, cultured in proliferation medium either with or without 50 nM givinostat, were incubated with 10 μM EdU for 16hrs. Following exposure, incubation with the reaction cocktail was performed for 30 min at room temperature. Afterward, cells were rinsed with PBS and mounted on microscope slides with FluoShield mounting medium (Invitrogen). cFAPs were similarly seeded and cultured for apoptosis detection achieved using the DeadEnd™ Fluorometric TUNEL System (Promega).

Images were acquired using a Leica DM6 B microscope and analyzed with ImageJ [27]. For each experimental condition, at least 10 randomly selected fields per coverslip were quantified.

2.6. RNA isolation

Total RNA was extracted from cultured cells using Trizol reagent (Invitrogen) following the manufacturer's instructions and resuspended in RNAse-free water. Its concentration was measured using a NanoDrop™ spectrophotometer (Thermo Fisher Scientific).

2.7. Bulk RNA-Sequencing

RNA-Sequencing was performed on four biological replicates of fibrogenic and adipogenic differentiated cells, with or without treatment with givinostat. At the end of the differentiation protocol, cells were collected in Trizol reagent (Invitrogen) and sent to BGI genomics technical service (China) where RNA was extracted, enriched for mRNA, and fragmented. cDNA was synthetized and ligated to adaptors. Sequencing was carried out using the BGISEQ sequencing platform, generating paired-end reads of 100 bp in length. Low quality reads were filtered out prior to data analysis. Clean reads were aligned to *Mus musculus* reference genome GCF_000001635.26_GRCm38.p6 using HISAT, while reference gene alignment was performed using Bowtie2. The average mapping ratio to the reference genome was 96,90 %, and the average mapping ratio to reference genes was 83,21 %. A total of 19.222 genes were identified. Genes with fewer than 10 counts in 3 samples for each condition within a given comparison were filtered out. Differentially expressed genes were determined using the edgeR R package with TMM normalization. Functional enrichment analysis, including Gene Ontology and pathway analysis, was performed using the clusterProfiler R package.

2.8. Retrotranscription and Real-time PCR

RNA was retrotranscribed into cDNA using the PrimeScript™ Reverse Transcriptase (Takara), following the manufacturer's protocol.

Real-time quantitative PCR (qPCR) was performed using PowerUp™ SYBR™ Green master mix (Applied Biosystems™ by Thermo Fisher Scientific) on a CFX384 Touch Real-Time PCR System (BioRad). Primers are listed in Table S1. Run data were analyzed using the BioRad CFX Manager™ software (BioRad), with further calculations performed in Excel (Microsoft). The TATA Binding Protein (*Tbp*) gene was used as a housekeeping gene for normalization. Relative quantifications between experimental conditions were calculated using the 2-ΔΔCt method. Analyses were performed independently for cFAPs obtained from WT or Tg-hQ mice. Graphs were generated using Prism 9 (Graphpad).

2.9. Protein extraction and western blot

Cells were lysed using complete RIPA buffer supplemented with 1X protease inhibitor (Roche) and 1X phosphatase inhibitor (Roche). Total protein concentration was quantified using the Pierce BCA protein assay kit (Thermo Fisher Scientific), following the manufacturer's instructions.

Protein extracts were separated by SDS–PAGE on precast 4–12 % Bis-Tris polyacrylamide gels (Invitrogen) and blotted onto nitrocellulose membranes using the Trans-Blot Turbo system (Bio-Rad). Membranes were blocked with 5 % milk in Tris-buffered saline (TBS) containing 0.05 % Tween and subsequently incubated overnight with primary antibodies (Table S2). Membranes were incubated with appropriate horseradish peroxidase-linked IgG (Jackson Immuno Research) for 1 h at room temperature. Bands were detected using the SuperSignal™ West Pico PLUS Chemiluminescent Substrate (Thermo Fisher Scientific). Membranes were visualized with the Alliance 9.7 Imaging System (UVItec Limited) and densitometric analysis was performed using ImageJ software.

2.10. Statistical analysis

Values in the graphs are presented as mean with standard error of the mean. Statistical analyses were performed with Prism 9 (GraphPad); statistical tests were selected based on the experimental design and are detailed in the figure legends. For datasets that were not-normally distributed, logarithmic transformation was applied prior to analysis.

3. Results

3.1. Transgenic mice show increased abundances of cFAPs number

cFAPs were isolated from the hearts of 10 month-old Tg-hQ mice, which at this age show cardiomyocyte loss and myocardial fibrosis, and control littermates through enzymatic digestion followed by FACS. Cell suspensions were labelled with antibodies against the pan-hematopoietic marker CD45, the endothelial marker CD31, the mesenchymal progenitor marker PDGFRα, and the stemness marker Sca1. cFAPs were identified as $CD45^-$ $CD31^-$ $PDGFR\alpha^+$. Sca-1 marker was used to distinguish between resting ($Sca1^+$) and committed ($Sca1^-$) cells, as previous studies have demonstrated that cFAPs lose Sca1 expression upon activation, concomitant with the acquisition of a more fibrotic phenotype [14]. The sorting strategy is summarized in Fig. 1A. We consistently observed a greater abundance of both resting and committed cFAPs in the hearts of Tg-hQ mice compared to WT, with the increase being particularly pronounced in the $Sca1^+$ population (Fig. 1B-C). All subsequent experiments were performed exclusively on the resting cFAP fraction.

3.2. Givinostat reduces cFAP proliferation in vitro

To confirm target engagement, we assessed whether givinostat altered global histone acetylation levels in cFAPs. Cells were cultured in proliferation medium with or without 50 nM givinostat for 3 and 6 h. Western blot analyses revealed a significant increase in histone H3 acetylation after 6 h of treatment, consistent with the expected inhibition of HDAC activity (Supplementary figure S1A-B).

We then investigated the effect of givinostat on cFAP proliferation using overnight EdU labelling. Freshly isolated cells were cultured in proliferation medium supplemented with or without 50 nM givinostat. No significant differences were observed in the proliferation rate of cFAPs derived from WT and Tg-hQ hearts. However, treatment with givinostat resulted in an approximately 40 % reduction of EdU-positive nuclei in both cell types, indicating a significant decrease in the number of cycling cells (Supplementary figure S1C-D). Notably, givinostat-treated cultures did not show an increase in apoptotic cells compared to untreated controls, as assessed by TUNEL assay (Supplementary figure S1E).

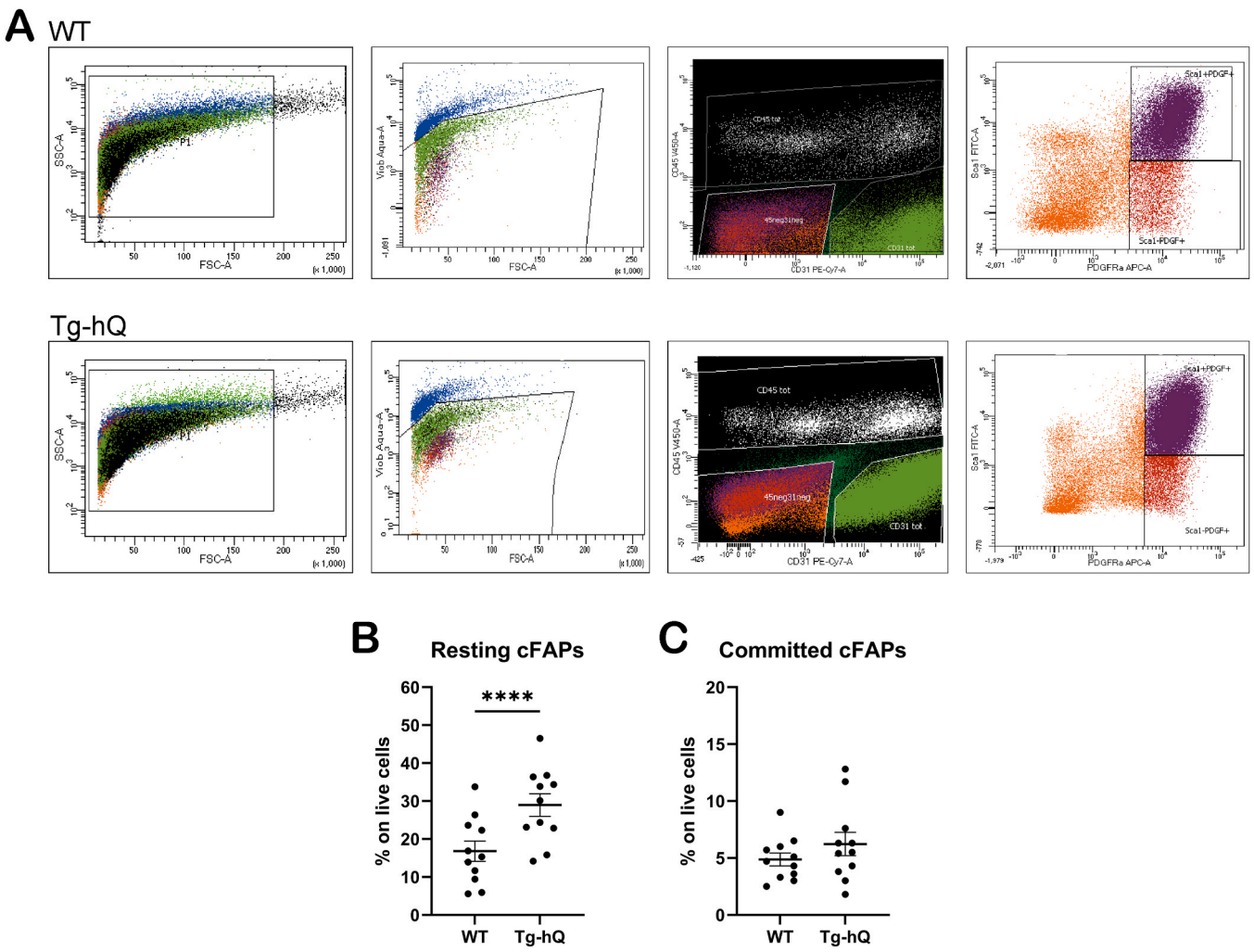

Fig. 1. Transgenic mice show increased abundances of cFAPs. (A) Flow cytometry plots showing the gating strategy used to isolate cFAPs from WT and Tg-hQ hearts. Positive gates were set by analyzing signals from FMO (Fluorescent Minus One) samples. Live non-myocyte cardiac cells were sorted to isolate cells positive for PDGFRα but negative for CD31 and CD45. Sca1 positivity was used to discriminate between resting (PDGFRα$^+$ Sca1$^+$) and committed (PDGFRα$^+$ Sca1$^-$) cFAPs. (B, C) Abundances of resting and committed cFAPs defined as the percentage on total live cells. Data are presented as mean±SEM; n = 11; parametric paired Student's *t*-test. *P < 0.05; **P < 0.01; ***P < 0.001.

3.3. Givinostat inhibits cFAP adipogenic differentiation in vitro

cFAPs from WT or Tg-hQ hearts were expanded for 3 days in proliferation medium and subsequently induced to differentiate into adipocytes using two sequential adipogenic media (AM I and AM II). Two experimental conditions were tested: cells were exposed either to 50 nM givinostat (AM + Giv) or to the vehicle alone (AM) (Fig. 2A). Regardless from their origin, cFAPs did not undergo spontaneous differentiation into adipocytes when cultured in standard proliferation medium (PM). Upon exposure to adipogenic stimuli, cFAPs differentiated into adipocytes, although differentiation efficiency varied across replicates (Fig. 2B-C). No significant differences were observed in the average number of adipocytes obtained from WT and transgenic-derived cFAPs under standard adipogenic conditions (Fig. 2C). Notably, the presence of givinostat during adipogenic differentiation significantly reduced the adipogenic potential of cFAPs, leading to approximatively 70 % fewer adipocytes per square cm, an effect observed consistently in both Tg-hQ and WT-derived cFAPs (Fig. 2C).

To investigate the transcriptional changes induced by givinostat during adipogenic differentiation, bulk RNA sequencing was performed on treated and untreated cells.

Comparison of transcriptomes between WT and Tg-hQ cells exposed to the adipogenic environment revealed only four differentially expressed genes (DEGs) (*Tagap*, *Rnaset2b*, *Rnaset2a, Scgb1a1*). When the comparison was applied to cells subjected to the differentiation protocol and treated with givinostat, three DEGs were identified (*Tagap*, *Rnaset2b*, *Nwd1*). These findings indicated a similar transcriptional response of WT and transgenic cFAPs under the same culture conditions.

In contrast, givinostat treatment significantly altered the transcriptomic profile of both WT and Tg-hQ cells compared to untreated controls. In WT cells, 744 DEGs were identified, with the majority being down-regulated (566) rather than up-regulated (178). In Tg-hQ cFAPs, 1002 DEGs were identified, of which 763 were down-regulated and 239 up-regulated upon treatment (Supplementary figure S2A-B).

Gene ontology (GO) analysis of DEGs from both WT and Tg-hQ cells revealed shared alterations in biological processes related to lipid metabolism. Indeed, fatty acids and triglyceride metabolic processes were ranked among the top 5 enriched terms (Fig. 2D, Supplementary figure S3). Notably, most genes associated with these pathways were downregulated in presence of the drug. Additionally, givinostat altered key adipogenic pathways, including the PPAR signaling pathway and the regulation of lipolysis in adipocytes (Fig. 2E, Supplementary figure S3). Consistent with these findings, key regulators of adipogenic activation (*Cebpa* and *Pparg)* and maturation (*Adipoq* and *Plin*) were significantly downregulated in treated cells compared to untreated controls (Supplementary figure S4). These transcriptional changes were

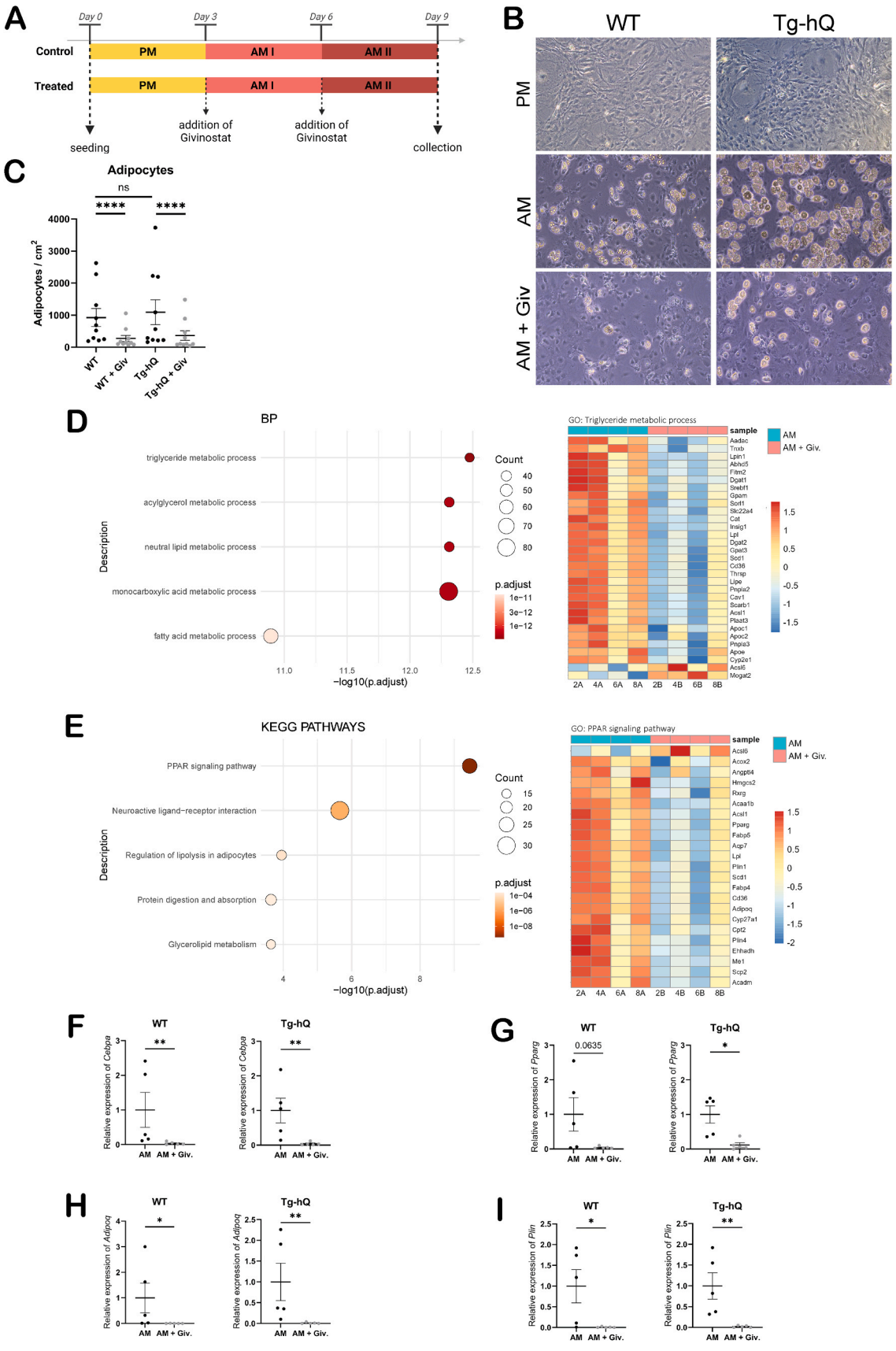

(caption on next page)

Fig. 2. Givinostat inhibits adipogenic differentiation. (A) Schematic representation of the workflow for adipogenic differentiation. (B) Representative bright-field microscope images of cells after 9 days of culture under different conditions. (C) Adipogenic potential evaluated as number of adipocytes per cm^2 obtained by exposing cFAPs to adipogenic stimulation in the presence or absence of 50 nM givinostat. n = 10. Data are presented as mean ± SEM; One-Way ANOVA with Tukey's correction for multiple comparisons. Outcomes of pairwise comparisons are shown only for biologically relevant comparisons. Logarithmic transformation was applied to raw data prior to statistical testing to ensure a Gaussian distribution. (D – E) Gene ontology (GO) terms associated with differentially expressed genes in treated versus untreated cells isolated from Tg-hQ mice. On the right: heat map with the genes associated with the most significant term of the corresponding GO. Each column represents data from a single biological replicate. The color scale bar represents the Z-score of gene expression. 2 A, 4 A, 6 A and 8 A: cells exposed to adipogenic differentiation. 2B, 4B, 6B and 8B: cells exposed to adipogenic differentiation and treated with 50 nM givinostat. BP: Biological Process. (F – I) Validation by Real Time qPCR of relevant adipogenic marker genes. *Cebpa*: CCAAT Enhancer Binding Protein Alpha; *Pparg*: peroxisome proliferator activated receptor gamma; *Adipoq*: Adiponectin; *Plin*: perilipin. Data are presented as mean±SEM; n = 5; Mann-Whitney test. ns: non-significative; *P < 0.05; **P < 0.01; ***P < 0.001. PM: Proliferation Medium; AM I: Adipogenic Medium I; AM II: Adipogenic Medium II; Giv: givinostat.

further validated on an independent sample set by RT-PCR, using *Tbp* as a housekeeping gene for normalization (Fig. 2F-I).

Taken together, these data demonstrate that givinostat inhibits adipogenic differentiation of cFAPs *in vitro*, which may be relevant to cardiac fatty accumulation observed in ACM.

3.4. Givinostat inhibits cFAP fibrogenic differentiation in vitro

cFAP differentiation into fibroblast was induced *in vitro* by supplementing the proliferation medium of both WT and Tg-hQ cells with 5 ng/mL TGFβ, with or without 50 nM givinostat treatment (Fig. 3A). To investigate the compound's effect at the transcriptomic level, bulk RNA

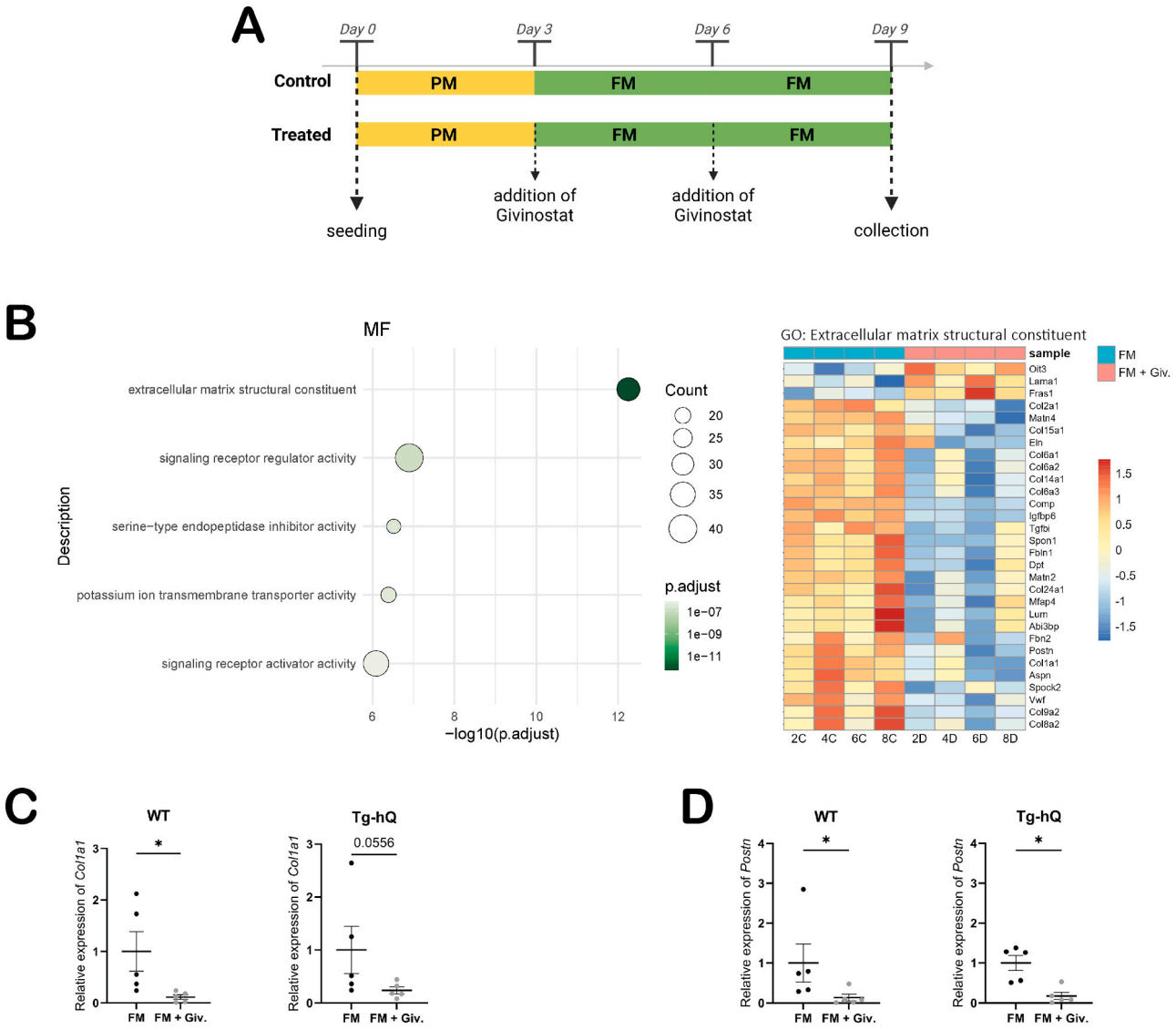

Fig. 3. Givinostat inhibits fibrotic differentiation. (A) Schematic representation of the workflow for fibrotic differentiation. (B) Gene ontology (GO) terms associated with differentially expressed genes in treated versus untreated cells isolated from Tg-hQ mice. On the right: heat map with genes associated with the most significant term of the corresponding GO. Each column represents data from a single biological replicate. The color scale bar represents the Z-score of gene expression. 2 C, 4 C, 6 C and 8 C: cells exposed to fibrogenic differentiation. 2D, 4D, 6D and 8D: cells exposed to fibrogenic differentiation and treated with 50 nM givinostat. MF: Molecular Function. (C – D) Validation by Real Time qPCR of relevant fibrogenic markers. *Col1a1*: Collagen type 1; *Postn*: Periostin. Data are presented as mean ± SEM; n = 5; Mann-Whitney test. *P < 0.05; **P < 0.01; ***P < 0.001. PM: Proliferation Medium; FM: Fibrogenic Medium; Giv: givinostat.

sequencing was performed. Tg-hQ and WT cells cultured under pro-fibrotic conditions exhibited highly similar transcriptomic profiles, with only three DEGs identified (*Tagap, Rnaset2b, Zfp965)*. Similarly, comparison between Tg-hQ and WT cells treated with the drug during fibrotic differentiation revealed four DEGs (*Tagap, Rnaset2b, H2ac19, Comp*). However, givinostat treatment induced significant transcriptomic changes in both Tg-hQ and WT cells compared to their untreated counterparts. In Tg-hQ cells, 698 DEGs were identified, with 257 genes upregulated and 441 genes downregulated. Similarly, in WT cells, 754 DEGs were detected, with 291 genes upregulated and 463 genes downregulated in treated versus untreated conditions (Supplementary figure S5A-B).

GO analysis, conducted separately for Tg-hQ and WT cells, identified the "extracellular matrix constituent" as the most enriched term in both cases (Fig. 3B, Supplementary figure S6).

Transcript levels of two representative ECM components, *Col1a1* and *Postn* were significantly reduced in the transcriptomic data (Supplementary figure S7A). These findings were validated by RT-PCR on an independent set of samples (Fig. 3C-D). Furthermore, immunoblotting confirmed the reduced production of Collagen I at the protein level (Supplementary figure S7B). Taken together, these results confirm the anti-fibrotic role of givinostat, consistent with previous *in vitro* and *in vivo* studies [26,28].

4. Discussion

The accumulation of fibro-fatty tissue progressively replacing the myocardium is a hallmark pathological process in ACM, contributing to the development of life-threatening ventricular arrhythmias and an increased risk of sudden cardiac death. Cardiomyocytes have traditionally been considered the primary cell population involved in ACM pathogenesis, as most pathogenic variants affect proteins involved in their mechano-functional junctions. However, the contribution of other cell types to ACM pathogenesis is now well recognized. Indeed, studies in murine models have proposed that reparative processes triggered by cardiomyocyte death rely on the activation of tissue-resident cardiac mesenchymal progenitors, characterized by the expression of Sca-1 and PDGFRα [14]. These progenitors, now referred to as FAP, were initially identified in skeletal muscle, where they positively influence muscle regeneration and homeostasis under physiological conditions [29–32]. Nonetheless, under chronic pathogenic conditions such as muscular dystrophy, FAPs are able to differentiate into fibroblasts and adipocytes, promoting fibrosis and fat deposition [33,34]. Similarly, PDGFRα^{+} progenitor cells capable of adipogenic and fibrogenic differentiation have also been identified in human skeletal muscles [35]. Given that Sca1 is a murine-specific antigen with no direct human homolog, alternative makers have been exploited to isolate these cells from human samples [36,37].

In the present study, both resting (Sca1^{+}) and committed (Sca1^{-}) cFAPs were found to be more abundant in the hearts of transgenic Tg-hQ mice compared to WT littermates, supporting their potential involvement in disease-associated cardiac remodeling. As the expression of the transgene in this model is under the control of the cardiac-specific mouse α-myosin heavy chain (α-MyHC) promoter, and therefore restricted to cardiomyocytes, the increased abundance of cFAPs may be explained by activating stimuli within the cardiac environment, rather than to a direct effect of the transgene on these cells. This observation is consistent with previous findings of FAP expansion in the *mdx* murine model of DMD, which occurs as a consequence of chronic muscle damage [33,34].

Given the relevant role that cFAPs may play in the development of fibro-fatty tissue in ACM, inhibiting their differentiation could represent a promising therapeutic approach to slowing disease progression. In this context, the pan HDACi givinostat demonstrated efficacy in reducing the activation of both primary adult rat ventricular fibroblasts and human ventricular fibroblasts, as well as their production of ECM components. Additionally, givinostat has been shown to block ECM remodeling, reduce ventricular stiffness in a murine model of diastolic dysfunction, and improve cardiac performance in a mouse model of acute myocardial infarction by attenuating cardiac fibrosis and inflammation [26,28].

In the present study, givinostat significantly reduced proliferation of both WT and Tg-hQ-derived cFAPs *in vitro,* without inducing cell death, consistent with previous studies on the antiproliferative effects of the compound. Notably, WT and Tg-hQ cFAPs exhibited similar proliferation rates, suggesting that isolation of these cells from their native environment may have eliminated initial differences.

It is well established that skeletal and cardiac FAPs can differentiate into fibroblasts or adipocytes *in vitro* when exposed to TGFβ [38] or adipogenic medium [38–40] respectively. In this study, givinostat significantly reduced the expression of several genes encoding collagen and other ECM components in cFAPs cultured in a pro-fibrotic environment, corroborating its previously reported anti-fibrotic effects [28].

Under adipogenic conditions, cFAPs differentiated into adipocytes with variable efficiency, and givinostat treatment effectively inhibited the adipogenic program. In line with previous studies on FAPs isolated from murine dystrophic muscle [38], adipogenic stimulation resulted in the up-pregulation of Peroxisome Proliferator-Activated Receptor gamma (PPARγ), a nuclear hormone receptor that plays a central role in promoting adipocyte differentiation and maturation, alongside its master regulator CCAAT/enhancer-binding proteins α (C/EBPα) [41]. In the current study, givinostat treatment significantly downregulated the expression of both *Pparg* and *Cebpa,* consistent with the observed reduction in adipocyte differentiation. Gene ontology analyses further identified the PPAR signaling pathway as one of the most down-regulated pathways in response to givinostat treatment in both WT and Tg-hQ cells. Beyond the downregulation of PPARγ, its transcriptional cofactor retinoid X receptor gamma (RXRG) and downstream targets such as adiponectin (ADIPOQ), perilipin (PLIN), lipoprotein lipase (LPL), and fatty acid translocase (FAT/CD36) were also significantly downregulated. This finding is particularly noteworthy, as two independent studies have reported activation of the PPAR pathway in cardiac samples from ACM patients carrying different ACM pathogenic variants [42,43].

Although cardiac adipogenesis is rarely observed in murine models, posing challenges for the direct validation of adipogenic inhibition *in vivo*, fatty accumulation in the heart remains a prominent feature of ACM. Therefore, the ability of givinostat to downregulate the PPAR pathway and suppress cFAP adipogenic differentiation *in vitro* underscores its potential as a therapeutic candidate for targeting this pathological feature of the disease.

The main limitation of this study is the absence of *in vivo* validation, which prevents direct conclusions on the therapeutic relevance of givinostat in ACM. No evidence is provided that the drug modulates disease-specific outcomes in the Tg-hQ model, such as myocardial fibro-fatty infiltration or alterations in cardiac structure and function. Moreover, the use of artificial differentiation protocols, although widely employed to assess cFAP plasticity, may not fully reproduce the myocardial microenvironment.

In conclusion, this study reports an increased proportion of cFAPs in the hearts of a transgenic ACM murine model compared to WT littermates. Independently of their source, cFAPs demonstrated similar differentiation potential equally into fibroblast and adipocytes *in vitro* under appropriate stimuli. Treatment with givinostat resulted in reduced proliferation and inhibition of fibro-fatty differentiation. These findings provide mechanistic evidence that givinostat can inhibit cFAP differentiation *in vitro*, laying the groundwork for future *in vivo* validation and potential therapeutic exploration.

CRediT authorship contribution statement

Chiara Romualdi: Formal analysis, Data curation. **Simonetta Andrea Licandro:** Writing – review & editing, Conceptualization.

Libero Vitiello: Writing – review & editing, Supervision, Methodology, Funding acquisition, Conceptualization. **Martina Calore:** Writing – review & editing, Funding acquisition, Conceptualization. **Alessandra Rampazzo:** Writing – review & editing, Writing – original draft, Visualization, Supervision, Project administration, Methodology, Funding acquisition, Conceptualization. **Chiara Romanato:** Investigation. **Christian Steinkuhler:** Writing – review & editing, Writing – original draft, Visualization, Supervision, Project administration, Methodology, Conceptualization. **Sara Vencato:** Writing – original draft, Visualization, Investigation, Formal analysis. **Monica Forino:** Writing – review & editing, Conceptualization. **Angelo Velle:** Formal analysis, Data curation. **Gianluca Fossati:** Writing – review & editing, Conceptualization. **Paola Braghetta:** Writing – review & editing, Funding acquisition, Conceptualization. **Nicola Facchinello:** Investigation.

Funding

The present study was supported by grants from the European Innovation Council (EIC) Pathfinder (IMPACT IMPACT-101115536 to A. R., M.C., L.V., P.B., C.S.,M.F., G.F., S.A.L.), Italian Ministry of University and Research (MUR) funded by the European Union – Next Generation EU (PRIN 2022HSJS4Y to A.R.), Cariparo Foundation (Starting Package C93C22008360007 to M.C.), European Union – Next Generation EU, Mission 4, Component 2, CUP B93D21010860004 (to A.R.), Telethon foundation grant (GMR24T1105 to M.C.), Beat the beat, La stella di Lorenzo onlus, Geca onlus.

Declaration of Competing Interest

The authors declare that they have no known competing financial interests or personal relationships that could have appeared to influence the work reported in this paper.

Appendix A. Supporting information

Supplementary data associated with this article can be found in the online version at doi:10.1016/j.biopha.2025.118549.

Data availability

Data will be made available on request.

References

[1] D. Corrado, M.S. Lin, H. Calkins, Arrhythmogenic right ventricular cardiomyopathy, N. Engl. J. Med. 376 (1) (2017) 61–72, https://doi.org/10.1056/nejmra1509267.
[2] G. Thiene, A. Nava, D. Corrado, L. Rossi, N. Pennelli, Right ventricular cardiomyopathy and sudden death in young people, N. Engl. J. Med. 318 (3) (1988) 129–133, https://doi.org/10.1056/nejm198801213180301.
[3] A. Nava, G. Thiene, B. Canciani, R. Scognamiglio, L. Daliento, G. Buja, B. Martini, P. Stritoni, G. Fasoli, Familial occurrence of right ventricular dysplasia: a study involving nine families, J. Am. Coll. Cardiol. 12 (5) (1988) 1222–1228, https://doi.org/10.1016/0735-1097(88)92603-4.
[4] N. Rastegar, S.L. Zimmerman, A.S.J.M. Te Riele, C. James, J.R. Burt, A. Bhonsale, B. Murray, C. Tichnell, D. Judge, H. Calkins, H. Tandri, D.A. Bluemke, I.R. Kamel, Spectrum of biventricular involvement on CMR among carriers of ARVD/C-associated mutations, JACC Cardiovasc. Imaging 8 (7) (2015) 863–864, https://doi.org/10.1016/j.jcmg.2014.09.009.
[5] B. Gerull, A. Brodehl, Insights into genetics and pathophysiology of arrhythmogenic cardiomyopathy, Curr. Heart Fail Rep. 18 (6) (2021) 378–390, https://doi.org/10.1007/s11897-021-00532-z.
[6] S.M. van der Voor, A.S.J.M. Te Riele, C. Basso, H. Calkins, C.A. Remme, T.A.B. van Veen, Arrhythmogenic cardiomyopathy: pathogenesis, pro-arrhythmic remodelling, and novel approaches for risk stratification and therapy, Cardiovasc. Res. 116 (9) (2020) 1571–1584, https://doi.org/10.1093/cvr/cvaa084.
[7] W.H. Bradford, J. Zhang, E.J. Gutierrez-Lara, Y. Liang, A. Do, T. Wang, L. Nguyen, N. Mataraarachchi, J. Wang, Y. Gu, J. Wang, Y. Gu, A. McCulloch, K.L. Peterson, F. Sheikh, Plakophilin 2 gene therapy prevents and rescues arrhythmogenic right ventricular cardiomyopathy in mouse model harboring patient genetics, Nat. Cardiovasc. Res. 2 (12) (2023) 1246–1261, https://doi.org/10.1038/s44161-023-00370-3.
[8] E. Kyriakopoulou, D. Versteeg, H. de Ruiter, I. Perini, F. Seibertz, Y. Döring, L. Zentilin, H. Tsui, S.J. van Kampen, M. Tiburcy, T. Meyer, N. Voigt, J.P. van Tintelen, W.H. Zimmermann, M. Giacca, E. van Rooij, Therapeutic efficacy of AAV-mediated restoration of PKP2 in arrhythmogenic cardiomyopathy, Nat. Cardiovasc Res 2 (12) (2023) 1262–1276, https://doi.org/10.1038/s44161-023-00378-9.
[9] C.J.M. van Opbergen, B. Narayanan, C.B. Sacramento, K.M. Stiles, V. Mishra, E. Frenk, D. Ricks, G. Chen, M. Zhang, P. Yarabe, J. Schwartz, M. Delmar, C. D. Herzog, M. Cerrone, AAV-Mediated delivery of Plakophilin-2a arrests progression of arrhythmogenic right ventricular cardiomyopathy in murine hearts: preclinical evidence supporting gene therapy in humans, Circ. Genom. Precis Med 17 (1) (2024) e004305, https://doi.org/10.1161/circgen.123.004305.
[10] E. Garcia-Gras, R. Lombardi, M.J. Giocondo, J.T. Willerson, M.D. Schneider, D. S. Khoury, A.J. Marian. suppression of canonical Wnt/beta-catenin signaling by nuclear plakoglobin recapitulates phenotype of arrhythmogenic right ventricular cardiomyopathy, J. Clin. Invest 116 (7) (2006) 2012–2021, https://doi.org/10.1172/jci27751.
[11] S.N. Chen, P. Gurha, R. Lombardi, A. Ruggiero, J.T. Willerson, A.J. Marian, The hippo pathway is activated and is a causal mechanism for adipogenesis in arrhythmogenic cardiomyopathy, Circ. Res 114 (3) (2014) 454–468, https://doi.org/10.1161/circresaha.114.302810.
[12] I. Stadiotti, V. Catto, M. Casella, C. Tondo, G. Pompilio, E. Sommariva, Arrhythmogenic cardiomyopathy: the guilty party in adipogenesis, J. Cardiovasc Transl. Res 10 (5-6) (2017) 446–454, https://doi.org/10.1007/s12265-017-9767-8.
[13] R. Lombardi, S.N. Chen, A. Ruggiero, P. Gurha, G.Z. Czernuszewicz, J.T. Willerson, A.J. Marian, Cardiac Fibro-Adipocyte progenitors express desmosome proteins and preferentially differentiate to adipocytes upon deletion of the desmoplakin gene, Circ. Res 119 (1) (2016) 41–54, https://doi.org/10.1161/circresaha.115.308136.
[14] H. Soliman, B. Paylor, R.W. Scott, D.R. Lemos, C. Chang, M. Arostegui, M. Low, C. Lee, D. Fiore, P. Braghetta, V. Pospichalova, C.E. Barkauskas, V. Korinek, A. Rampazzo, K. MacLeod, T.M. Underhill, F.M.V. Rossi, Pathogenic potential of Hic1-Expressing cardiac stromal progenitors, Cell Stem Cell 26 (6) (2020) 205–220, https://doi.org/10.1016/j.stem.2019.12.008.
[15] M. Calore, A. Lorenzon, L. Vitiello, G. Poloni, M.A.F. Khan, G. Beffagna, E. Dazzo, C. Sacchetto, R. Polishchuk, P. Sabatelli, R. Doliana, D. Carnevale, G. Lembo, P. Bonaldo, L. De Windt, P. Braghetta, A. Rampazzo, A novel murine model for arrhythmogenic cardiomyopathy points to a pathogenic role of wnt signalling and miRNA dysregulation, Cardiovasc Res 115 (4) (2019) 739–751, https://doi.org/10.1093/cvr/cvy253.
[16] X. Lyu, M. Hu, J. Peng, X. Zhang, Y.Y. Sanders, HDAC inhibitors as antifibrotic drugs in cardiac and pulmonary fibrosis, 2040622319862697, Ther. Adv. Chronic Dis. 10 (2019), https://doi.org/10.1177/2040622319862697.
[17] T.G. Gillette, J.A. Hill, Readers, writers, and erasers: chromatin as the whiteboard of heart disease, Circ. Res 116 (7) (2015) 1245–1253, https://doi.org/10.1161/circresaha.116.303630.
[18] S. Consalvi, C. Mozzetta, P. Bettica, M. Germani, F. Fiorentini, F. Del Bene, M. Rocchetti, F. Leoni, V. Monzani, P. Mascagni, P.L. Puri, V. Saccone, Preclinical studies in the mdx mouse model of duchenne muscular dystrophy with the histone deacetylase inhibitor givinostat, Mol. Med 19 (1) (2013) 79–87, https://doi.org/10.2119/molmed.2013.00011.
[19] S.A. Licandro, L. Crippa, R. Pomarico, R. Perego, G. Fossati, F. Leoni, C. Steinkühler, The pan HDAC inhibitor givinostatimproves muscle function and histological parameters in two duchenne muscular dystrophy murine models expressing different haplotypes of the LTBP4 gene, Skelet. Muscle 11 (1) (2021) 19, https://doi.org/10.1186/s13395-021-00273-6.
[20] P. Bettica, S. Petrini, V. D'Oria, A. D'Amico, M. Catteruccia, M. Pane, S. Sivo, F. Magri, S. Brajkovic, S. Messina, G.L. Vita, B. Gatti, M. Moggio, P.L. Puri, M. Rocchetti, G. De Nicolao, G. Vita, G.P. Comi, E. Bertini, E. Mercuri, Histological effects of givinostatin boys with duchenne muscular dystrophy, Neuromuscul. Disord. 26 (10) (2016) 643–649, https://doi.org/10.1016/j.nmd.2016.07.002.
[21] E. Mercuri, J.J. Vilchez, O. Boespflug-Tanguy, C.M. Zaidman, J.K. Mah, N. Goemans, W. Müller-Felber, E.H. Niks, U. Schara-Schmidt, E. Bertini, G.P. Comi, K.D. Mathews, L. Servais, K. Vandenborne, J. Johannsen, S. Messina, S. Spinty, L. McAdam, K. Selby, B. Byrne, C.G. Laverty, K. Carroll, G. Zardi, S. Cazzaniga, N. Coceani, P. Bettica, C.M. McDonald, EPIDYS study group. Safety and efficacy of givinostat in boys with duchenne muscular dystrophy (EPIDYS): a multicentre, randomised, double-blind, placebo-controlled, phase 3 trial, Lancet Neurol. 23 (4) (2024) 393–403, https://doi.org/10.1016/s1474-4422(24)00036-x.
[22] ⟨https://www.fda.gov/news-events/press-announcements/fda-approves-nonsteroidal-treatment-duchenne-muscular-dystrophy⟩.
[23] C. Mozzetta, V. Sartorelli, C. Steinkuhler, P.L. Puri, HDAC inhibitors as pharmacological treatment for duchenne muscular dystrophy: a discovery journey from bench to patients, Trends Mol. Med 30 (3) (2024) 278–294, https://doi.org/10.1016/j.molmed.2024.01.007.
[24] Y. Kong, P. Tannous, G. Lu, K. Berenji, B.A. Rothermel, E.N. Olson, J.A. Hill, Suppression of class I and II histone deacetylases blunts pressure-overload cardiac hypertrophy, Circulation 113 (22) (2006) 2579–2588, https://doi.org/10.1161/circulationaha.106.625467.
[25] J. Liu, W. Fu, X. Wang, Z. Liang, F. Meng, The role of HDAC2 inhibition in cardioprotection against doxorubicin-induced myocardial injury, Front Cardiovasc Med 12 (2025) 1557119, https://doi.org/10.3389/fcvm.2025.1557119.
[26] M. Milan, V. Pace, F. Maiullari, M. Chirivì, D. Baci, S. Maiullari, L. Madaro, S. Maccari, T. Stati, G. Marano, G. Frati, P.L. Puri, E. De Falco, C. Bearzi, R. Rizzi, Givinostat reduces adverse cardiac remodeling through regulating fibroblasts activation, Cell Death Dis. 9 (2) (2018) 108, https://doi.org/10.1038/s41419-017-0174-5.

[27] C.A. Schneider, W.S. Rasband, K.W. Eliceiri, NIH image to ImageJ: 25 years of image analysis, Nat. Methods 9 (7) (2012) 671–675, https://doi.org/10.1038/nmeth.2089.
[28] J.G. Travers, S.A. Wennersten, B. Peña, R.A. Bagchi, H.E. Smith, R.A. Hirsch, L. A. Vanderlinden, Y.H. Lin, E. Dobrinskikh, K.M. Demos-Davies, M.A. Cavasin, L. Mestroni, C. Steinkühler, C.Y. Lin, S.R. Houser, K.C. Woulfe, M.P.Y. Lam, T. A. McKinsey, HDAC inhibition reverses preexisting diastolic dysfunction and blocks covert extracellular matrix remodeling, Circulation 143 (19) (2021) 1874–1890, https://doi.org/10.1161/circulationaha.120.046462.
[29] A. Uezumi, S. Fukada, N. Yamamoto, S. Takeda, K. Tsuchida, Mesenchymal progenitors distinct from satellite cells contribute to ectopic fat cell formation in skeletal muscle, Nat. Cell Biol. 12 (2) (2010) 143–152, https://doi.org/10.1038/ncb2014.
[30] A.W.B. Joe, L. Yi, A. Natarajan, F. Le Grand, L. So, J. Wang, M.A. Rudnicki, F.M. V. Rossi, Muscle injury activates resident fibro/adipogenic progenitors that facilitate myogenesis, Nat. Cell Biol. 12 (2) (2010) 153–163, https://doi.org/10.1038/ncb2015.
[31] M.N. Wosczyna, C.T. Konishi, E.E. Perez Carbajal, T.T. Wang, R.A. Walsh, Q. Gan, M.W. Wagner, T.A. Rando, Mesenchymal stromal cells are required for regeneration and homeostatic maintenance of skeletal muscle, Cell Rep. 27 (7) (2019) 2029–2035, https://doi.org/10.1016/j.celrep.2019.04.074.
[32] X. Kang, K. Zhao, Z. Huang, S.I. Fukada, X.W. Qi, H. Miao, Pdgfrα+ stromal cells, a key regulator for tissue homeostasis and dysfunction in distinct organs, Genes Dis. 12 (2) (2024) 101264, https://doi.org/10.1016/j.gendis.2024.101264.
[33] A. Uezumi, T. Ito, D. Morikawa, N. Shimizu, T. Yoneda, M. Segawa, M. Yamaguchi, R. Ogawa, M.M. Matev, Y. Miyagoe-Suzuki, S. Takeda, K. Tsujikawa, K. Tsuchida, H. Yamamoto, S. Fukada, Fibrosis and adipogenesis originate from a common mesenchymal progenitor in skeletal muscle, J. Cell Sci. 124 (Pt21) (2011) 3654–3664, https://doi.org/10.1242/jcs.086629.
[34] D.R. Lemos, F. Babaeijandaghi, M. Low, C.K. Chang, S.T. Lee, D. Fiore, R.H. Zhang, A. Natarajan, S.A. Nedospasov, F.M.V. Rossi, Nilotinib reduces muscle fibrosis in chronic muscle injury by promoting TNF-mediated apoptosis of fibro/adipogenic progenitors, Nat. Med 21 (7) (2015) 786–794, https://doi.org/10.1038/nm.3869.
[35] A. Uezumi, S. Fukada, N. Yamamoto, M. Ikemoto-Uezumi, M. Nakatani, M. Morita, A. Yamaguchi, H. Yamada, I. Nishino, Y. Hamada, K. Tsuchida, Identification and characterization of PDGFRα+ mesenchymal progenitors in human skeletal muscle, Cell Death Dis. 5 (4) (2014) e1186, https://doi.org/10.1038/cddis.2014.161.
[36] N. Arrighi, C. Moratal, N. Clément, S. Giorgetti-Peraldi, P. Peraldi, A. Loubat, J. Y. Kurzenne, C. Dani, A. Chopard, C.A. Dechesne, Characterization of adipocytes derived from fibro/adipogenic progenitors resident in human skeletal muscle, Cell Death Dis. 6 (4) (2015) e1733, https://doi.org/10.1038/cddis.2015.79.
[37] J. Farup, J. Just, F. de Paoli, L. Lin, J.B. Jensen, T. Billeskov, I.S. Roman, C. Cömert, A.B. Møller, L. Madaro, E. Groppa, R.G. Fred, U. Kampmann, L.C. Gormsen, S. B. Pedersen, P. Bross, T. Stevnsner, N. Eldrup, T.H. Pers, F.M.V. Rossi, P.L. Puri, N. Jessen, Human skeletal muscle CD90+ fibro-adipogenic progenitors are associated with muscle degeneration in type 2 diabetic patients, e11, Cell Metab. 33 (11) (2021) 2201–2214, https://doi.org/10.1016/j.cmet.2021.10.001.
[38] A. Reggio, M. Rosina, A. Palma, A. Cerquone Perpetuini, L.L. Petrilli, C. Gargioli, C. Fuoco, E. Micarelli, G. Giuliani, M. Cerretani, A. Bresciani, F. Sacco, L. Castagnoli, G. Cesareni, Adipogenesis of skeletal muscle fibro/adipogenic progenitors is affected by the WNT5a/GSK3/β-catenin axis, Cell Death Differ. 27 (10) (2020) 2921–2941, https://doi.org/10.1038/s41418-020-0551-y.
[39] R. Lombardi, M. da Graca Cabreira-Hansen, A. Bell, R.R. Fromm, J.T. Willerson, A. J. Marian, Nuclear plakoglobin is essential for differentiation of cardiac progenitor cells to adipocytes in arrhythmogenic right ventricular cardiomyopathy, Circ. Res. 109 (12) (2011) 1342–1353, https://doi.org/10.1161/circresaha.111.255075.
[40] M. Marinkovic, C. Fuoco, F. Sacco, A. Cerquone Perpetuini, G. Giuliani, E. Micarelli, T. Pavlidou, L.L. Petrilli, A. Reggio, F. Riccio, F. Spada, S. Vumbaca, A. Zuccotti, L. Castagnoli, M. Mann, C. Gargioli, G. Cesareni, Fibro-adipogenic progenitors of dystrophic mice are insensitive to NOTCH regulation of adipogenesis, Life Sci. Alliance 2 (3) (2019) e201900437, https://doi.org/10.26508/lsa.201900437.
[41] E.D. Rosen, C.H. Hsu, X. Wang, S. Sakai, M.W. Freeman, F.J. Gonzalez, B. M. Spiegelman, C/EBPalpha induces adipogenesis through PPARgamma: a unified pathway, Genes Dev. 16 (1) (2002) 22–26, https://doi.org/10.1101/gad.948702.
[42] F. Djouadi, Y. Lecarpentier, J.L. Hébert, P. Charron, J. Bastin, C. Coirault, A potential link between peroxisome proliferator-activated receptor signalling and the pathogenesis of arrhythmogenic right ventricular cardiomyopathy, Cardiovasc. Res. 84 (1) (2009) 83–90, https://doi.org/10.1093/cvr/cvp183.
[43] J.B. Reisqs, A. Moreau, A. Charrabi, Y. Sleiman, A.C. Meli, G. Millat, V. Briand, P. Beauverger, S. Richard, P. Chevalier, The PPARγ pathway determines electrophysiological remodelling and arrhythmia risks in DSC2 arrhythmogenic cardiomyopathy, Clin. Transl. Med. 12 (3) (2022) e748, https://doi.org/10.1002/ctm2.748.